AIMS Mathematics, 8(9): 21191–21207.
DOI:10.3934/math.20231080
Received: 06 May 2023
Revised: 10 June 2023
Accepted: 15 June 2023
Published: 03 July 2023

http://www.aimspress.com/journal/Math

Research article

Complete study of local convergence and basin of attraction of sixth-order iterative method

Kasmita Devi and Prashanth Maroju*

Department of Mathematics, SAS, VIT-AP University, Amaravati 522237, Andhra Pradesh, India

* **Correspondence:** Email: maroju.prashanth@gmail.com; Tel: 8309592957.

Abstract: The local convergence analysis of the parameter based sixth-order iterative method is the primary focus of this article. This investigation was conducted based on the Fréchet derivative of the first order that satisfies the Lipschitz continuity condition. In addition, we developed a conceptual radius of convergence for these methods. Also, we discussed the solution behavior of complex polynomials with the basin of attraction. Finally, some numerical examples are provided to illustrate how the conclusions we got can be employed to determine the iterative approach's radius of convergence ball in the context of solving nonlinear equations. We compare the numerical results with our method and the existing sixth order methods proposed by Argyros et al. We observe that using our method yields significantly larger balls than those that already exist.

Keywords: local convergence; basin of attraction; nonlinear equations; Lipschitz continuity condition; Fréchet derivative
Mathematics Subject Classification: 65H10

1. Introduction

In applied sciences and engineering, many problems can be represented by a nonlinear equation or system of nonlinear equations [1–3]. To solve these types of nonlinear equations we have some iterative methods in numerical analysis. For solving nonlinear equations, numerous researchers came up with iterative procedures of higher order. Additionally, they discussed the convergence analysis of extending these techniques to Banach space. The nonlinear problems naturally appear as follows:

$$\Psi(\phi) = 0 \tag{1.1}$$

where $\Psi : \Omega \subset S \to S$, given that $\Omega \subseteq S$ is nonempty open convex and S is a Banach space.

The study of the convergence analysis of iterative methods is usually divided into two categories: semilocal convergence and local convergence. Semilocal convergence of iterative methods are

discussed with two approches, i.e, the use of recurrence relations and majorizing sequences. The goal of the semilocal convergence is to provide criteria guaranteeing the convergence of iteration procedures utilizing information around an initial point while the purpose of local convergence is to find estimates of the computed radii of the convergence balls which is based on the information around a solution ϕ^* [4]. The convergence domain is a key issue in the study of iterative procedures. In most cases, the convergence domain is quite small. Thus, it is crucial to increase the convergence domain without introducing new hypotheses. The need for better error estimates for the distances $\|\phi_{n+1} - \phi_n\|$ and $\|\phi_n - \phi^*\|$ is another pressing issue. Newton's method has been shown to converge on Banach spaces by Kantorovich and Akilov [5]. The convergence of Newton's method was proved by Rall [6] using recurrence relations. A similar strategy was used to prove local convergence of higher-order methods in Banach spaces by several researchers [7–14]. In the literature, we have found several higher-order iterative methods, and the local and semilocal convergence of those methods has been discussed by many researchers. The local convergence of the fifth order method is discussed in [10, 11, 14]. The local convergence of the sixth order method was established by researchers in [7–9, 13].

Sharma et al. in [15] developed the fourth-order iterative method as follows:

$$\begin{cases} \psi_n = \phi_n - \frac{2}{3}\Big(\Psi'(\phi_n)\Big)^{-1}\Psi(\phi_n), \\ \phi_{n+1} = \phi_n - \frac{1}{2}\Big[- I + \frac{9}{4}\Big(\Psi'(\psi_n)\Big)^{-1}\Big(\Psi'(\phi_n) + \frac{3}{4}\Big(\Psi'(\phi_n)\Big)^{-1} \\ \quad \Big(\Psi'(\psi_n)\Big)^{-1}\Big]\Big(\Psi'(\phi_n)\Big)^{-1}\Psi(\phi_n). \end{cases} \tag{1.2}$$

Soleymani in [16] developed the fourth-order iterative method as follows:

$$\begin{cases} \psi_n = \phi_n - \frac{2}{3}\Big(\Psi'(\phi_n)\Big)^{-1}\Psi(\phi_n), \\ \phi_{n+1} = \phi_n - \Big[I - \frac{3}{8}\Big[I - \Big(\Psi'(\psi_n)\Big)^{-1}\Big(\Psi'(\phi_n)\Big)^{-1} + \frac{3}{4}\Big(\Psi'(\phi_n)\Big)^{-1} \\ \quad \Big(\Psi'(\psi_n)\Big)^{-1}\Big]\Big(\Psi'(\phi_n)\Big)^{-1}\Psi(\phi_n). \end{cases} \tag{1.3}$$

Montazeri et al. in [2] developed the sixth-order iterative method from Eqs (1.2) and (1.3) :

$$\begin{cases} \psi_n = \phi_n - \frac{2}{3}\Big(\Psi'(\phi_n)\Big)^{-1}\Psi(\phi_n), \\ z_n = \phi_n - \Big[\frac{23I}{8} - 3\Big[I - \Big(\Psi'(\psi_n)\Big(\Psi'(\phi_n)\Big)^{-1} + \frac{9}{8}\Big(\Big(\Psi'(\phi_n)\Big)^{-1} \\ \quad \Psi'(\psi_n)\Big)^2\Big]\Big(\Psi'(\phi_n)\Big)^{-1}\Psi(\phi_n), \\ \phi_{n+1} = z_n - \Big[\frac{5}{2}I - \frac{3}{2}\Big(\Psi'(\phi_n)\Big)^{-1}\Psi'(\psi_n)\Big]\Big(\Psi'(\phi_n)\Big)^{-1}\Psi(z_n). \end{cases} \tag{1.4}$$

Chun and Neta in [1] developed the weight function approch for sixth-order iterative methods of

Eq (1.4) as follows:

$$\begin{cases} \psi_n = \phi_n - w_1(\Psi'(\phi_n))^{-1}\Psi(\phi_n), \\ z_n = \phi_n - W_1(\phi_n, \psi_n)(\Psi'(\phi_n))^{-1}\Psi(\phi_n), \\ \phi_{n+1} = z_n - W_2(\phi_n, \psi_n)(\Psi'(\phi_n))^{-1}\Psi(z_n). \end{cases} \tag{1.5}$$

$$w_1 = \frac{2}{3}, W_1(\phi_n, \psi_n) = a_1 I + a_2 s_n + a_3 t_n + a_4 (s_n)^2 + a_5 (t_n)^2 + a_6 (t_n)^3,$$
$$W_2(\phi_n, \psi_n) = b_1 I + b_2 s_n + b_3 t_n + b_4 (s_n)^2 + b_5 (t_n)^2,$$

where $t_n = \left[\Psi'(\phi_n)\right]^{-1}\Psi'(\psi_n)$, $s_n = \left[\Psi'(\psi_n)\right]^{-1}\Psi'(\phi_n)$.

This paper's primary objective was motivated by recent research on the local convergence of the sixth-order iterative method (1.5) in Banach spaces. The local convergence analysis is discussed by employing first-order Fréchet derivatives satisfying the Lipschitz condition in Banach spaces. An existence and uniqueness theorem is conclusively demonstrated under these conditions. The established theorem is then used to calculate the radii of convergence balls in a number of worked-out examples. The basin of attraction in complex planes is discussed.

The rest of the paper is structured as follows: In Section 2, the iterative method's local convergence analysis is described. In Section 3, we present the basin of attraction. The numerical examples are shown in Section 4, and the concluding remarks are given in Section 5.

2. Local convergence

In this section, we present local convergence analysis of the method represented by Eq (1.5). Let $\mho(\upsilon, r), \overline{\mho}(\upsilon, r)$ stand for the open and closed balls in S, respectively, with a center $\upsilon \in S$ of radius $r > 0$. Let $\mu_0, \mu, \kappa > 0$ and $\alpha \in S$ be given parameters with $\mu_0 \leq \mu$. On the interval $[0, \frac{1}{\mu_0})$ define the function ρ_1 by

$$\rho_1(t) = \frac{\mu t}{2(1 - \mu_0 t)}. \tag{2.1}$$

On the interval $[0, \frac{1}{\mu_0})$ define the functions ρ_2 and h_2 by

$$\rho_2(t) = \frac{\mu}{2(1 - \mu_0 t)} + |3|\left(\frac{1}{1 - \mu_0 t}\right)^2 \kappa^2 \rho_1(t) + \left|-\frac{9}{8}\right|\left(\frac{1}{1 - \mu_0 t}\right)^3 \kappa^3 \rho_1(t),$$

and

$$h_2(t) = \rho_2(t) - 1. \tag{2.2}$$

Also, we define the function $\rho_3(t)$, $h_3(t)$ on the interval $(0, r_2)$ by

$$\rho_3(t) = \rho_2 + \left|-\frac{5}{2}\right| \kappa \rho_2 \frac{1}{1 - \mu_0 t} + \frac{3}{2}\kappa^2 \rho_2 \left(\frac{1}{1 - \mu_0 t}\right)^2,$$

$$h_3(t) = \rho_3(t) - 1, \tag{2.3}$$

and

$$r = \min(r_1, r_2, r_3) < \frac{1}{\mu_0}. \tag{2.4}$$

Then, we have for each $t \in [0, r)$,

$$0 \leq \rho_1(t) < 1, \tag{2.5}$$

$$0 \leq \rho_2(t) < 1, \tag{2.6}$$

$$0 \leq \rho_3(t) < 1. \tag{2.7}$$

Theorem 2.1. *Let $\Psi : \Omega \subset S \to S$ be a differentiable function. Suppose that there exists $\phi^* \in \Omega$, that $\mu_0 > 0, \mu > 0$ and $\kappa \geq 1$ are the given parameters and for each $\phi, \psi \in \Omega$ the following is true:*

$$\Psi(\phi^*) = 0, (\Psi'(\phi^*))^{-1} \in L(S, S),$$

$$\|\Psi'(\phi^*)^{-1}(\Psi'(\phi) - \Psi'(\phi^*))\| \leq \mu_0\|\phi - \phi^*\|, \tag{2.8}$$

$$\|\Psi'(\phi^*)^{-1}(\Psi'(\phi) - \Psi'(\psi)\| \leq \mu\|\phi - \psi\|, \tag{2.9}$$

$$\|\Psi'(\phi^*)^{-1}\Psi'(\phi)\| \leq \kappa, \tag{2.10}$$

and

$$\overline{\mho}(\phi^*, r) \subseteq \Omega. \tag{2.11}$$

Then the sequence converges to ϕ^*, as generated by the method given by the Eq (1.5) for $\phi_0 \in \mho(\phi^*, r) \setminus \phi^*$, which is well defined in $\overline{\mho}(\phi^*, r)$ for each $n = 0, 1, 2, 3, \ldots$, where r is given by Eq (2.4). Moreover the following estimates hold:

$$\|\psi_n - \phi^*\| \leq \rho_1(\|(\phi_n - \phi^*\|))\|(\phi_n - \phi^*)\| < \|(\phi_n - \phi^*)\| < 1, \tag{2.12}$$

$$\|z_n - \phi^*\| \leq \rho_2(\|(\phi_n - \phi^*\|))\|(\phi_n - \phi^*)\| < \|(\phi_n - \phi^*)\| < 1, \tag{2.13}$$

$$\|\phi_{n+1} - \phi^*\| \leq \rho_3(\|(\phi_n - \phi^*\|))\|(\phi_n - \phi^*)\| < \|(\phi_n - \phi^*)\| < 1. \tag{2.14}$$

Furthermore, suppose that there exists $R \in [r, \frac{2}{L_0})$ such that $\overline{\mho}(\phi^*, R)$; then, the limit point ϕ^* is the only solution of $\Psi(\phi) = 0$ in $\overline{\mho}(\phi^*, R)$.

Proof. Let $\Psi : \Omega \subseteq S \to S$ be a Fréchet differentiable operator. In the domain Ω, suppose that ϕ^* is the solution and $\phi^* \in \Omega$, and that ϕ_0 is the initial point and $\phi_0 \in \Omega$.
From the condition given by Eq (2.8),

$$\|\Psi'(\phi^*)^{-1}(\Psi'(\phi) - \Psi'(\phi^*))\| \leq \mu_0\|\phi - \phi^*\|.$$

For $\phi_0 \in \Omega$, we have

$$\|\Psi'(\phi^*)^{-1}(\Psi'(\phi_0) - \Psi'(\phi^*))\| \leq \mu_0\|\phi_0 - \phi^*\|. \tag{2.15}$$

Consider that $\|\phi_0 - \phi^*\| < \frac{1}{\mu_0}$ and

$$\|\Psi'(\phi^*)^{-1}(\Psi'(\phi_0) - \Psi'(\phi^*))\| < 1.$$

Hence, we get

$$\|I - \Psi'(\phi^*)^{-1}\Psi'(\phi_0)\| < 1. \tag{2.16}$$

From this, by the Banach lemma, $(\Psi'(\phi_0))^{-1}$ exists and $(\Psi'(\phi_0))^{-1} \in L(S, S)$, where $L(S, S)$ is set of all bounded linear operators from S to S.

$$\|(\Psi'(\phi_0))^{-1}\Psi'(\phi)^*\| \leq \frac{1}{1-\mu_0\|\phi_0-\phi^*\|}. \tag{2.17}$$

We prove this theorem by using mathematical induction. For $n = 0$, from step one of the method given by Eq (1.5), we have

$$\psi_0 - \phi^* = -(\Psi'(\phi_0))^{-1}\int_0^1 \left[\Psi'(\phi^* + \theta(\phi_0-\phi^*)) - \Psi'(\phi_0)\right] d\theta(\phi_0-\phi^*). \tag{2.18}$$

Taking the norm on both sides of Eq (2.18), we get

$$\begin{aligned}
\|\psi_0-\phi^*\| &\leq \|(\Psi'(\phi_0))^{-1}\int_0^1 \left[\Psi'(\phi^* + \theta(\phi_0-\phi^*)) - \Psi'(\phi_0)\right] d\theta(\phi_0-\phi^*)\| \\
&\leq \frac{\mu\|(\phi_0-\phi^*)\|^2}{2(1-\mu_0\|(\phi_0-\phi^*)\|)} \\
&\leq \rho_1(\|(\phi_0-\phi^*))\|)\|(\phi_0-\phi^*).
\end{aligned}$$

Hence, $\psi_0 \in \mho(\phi^*, r)$, where,

$$\rho_1(t) = \frac{\mu t}{2(1-\mu_0 t)}. \tag{2.19}$$

Now, from the second step of the method, we have

$$z_0-\phi^* = \phi_0-\phi^* - \frac{23}{8}(\Psi'(\phi_0))^{-1}\Psi(\phi_0) + 3(\Psi'(\phi_0))^{-2}\Psi'(\psi_0)\Psi(\phi_0) - \frac{9}{8}(\Psi'(\phi_0))^{-3}\Psi'(\psi_0)^2\Psi(\phi_0). \tag{2.20}$$

Applying the norm on both sides, we get

$$\begin{aligned}
\|z_0-\phi^*\| &\leq \|\phi_0-\phi^*-(\Psi'(\phi_0))^{-1}\Psi(\phi_0)\| + |3|\,\|(\Psi'(\phi_0))^{-2}\Psi'(\psi_0)\Psi(\phi_0\| + \left|-\frac{9}{8}\right|\|(\Psi'(\phi_0))^{-3}\Psi'(\psi_0)^2\Psi(\phi_0)\| \\
&\leq \frac{\mu}{2(1-\mu_0\|(\phi_0-\phi^*)\|)} + |3|\left(\frac{1}{1-\mu_0\|(\phi_0-\phi^*))\|}\right)^2\kappa^2\rho_1(\|(\phi_0-\phi^*)\|) + \\
&\quad \left|-\frac{9}{8}\right|\left(\frac{1}{1-\mu_0\|(\phi_0-\phi^*))\|}\right)^3\kappa^3\rho_1(\|(\phi_0-\phi^*)\|) \\
&\leq \rho_2(\|(\phi_0-\phi^*)\|)\|(\phi_0-\phi^*)\| < \|(\phi_0-\phi^*)\| < r,
\end{aligned}$$

where

$$\rho_2(t) = \frac{\mu}{2(1-\mu_0(t))} + |3|\left(\frac{1}{1-\mu_0(t)}\right)^2\kappa^2\rho_1(t) + \left|-\frac{9}{8}\right|\left(\frac{1}{1-\mu_0(t)}\right)^3\kappa^3\rho_1(t). \tag{2.21}$$

From the third step of the method, we have

$$\phi_1 = z_0 - \frac{5}{2}(\Psi'(\phi_0))^{-1}\Psi(z_0) + \frac{3}{2}(\Psi'(\phi_0))^{-2}\Psi(z_0)\Psi'(\psi_0). \tag{2.22}$$

By Applying the norm, we get

$$\begin{aligned}\|\phi_1-\phi^*\| &= \|z_0-\phi^*\|+\left|-\frac{5}{2}\right|\|\Psi'(\phi_0))^{-1}\Psi'(\phi^*)\|\|\Psi(z_0)\Psi'(\phi^*)^{-1}\| \\ &\quad +\frac{3}{2}\|(\Psi'(\phi_0))^{-2}(\Psi'(\phi^*))^2\|\|\Psi(z_0)\Psi'(\phi^*)^{-1}\|\|\Psi'(\psi_0)\Psi'(\phi^*)^{-1}\| \\ &\leq \rho_3(\|(\phi_0-\phi^*)\|)\|(\phi_0-\phi^*)\|,\end{aligned}$$

where

$$\rho_3=\rho_2(t)+\left|-\frac{5}{2}\right|\kappa\rho_2(t)\frac{1}{1-\mu_0 t}+\frac{3}{2}\kappa^2\rho_2(t)\left(\frac{1}{1-\mu_0 t}\right)^2. \tag{2.23}$$

From this, we can conclude that $\phi_1 \in \mho(\phi^*, r)$ for $n = 0$. By induction, replacing ϕ_0, ψ_0, z_0 and ϕ_1 by ϕ_k, ψ_k, z_k and ϕ_{k+1}, respectively, in the following estimates, we arrive at Eqs (2.12)–(2.14). Using the estimate, $\|\phi_{k+1}-\phi^*\| < \|\phi_k-\phi^*\| < r$.

We deduce that $lim_{n\to\infty}\phi_k = \phi^*$ and $\phi_{k+1} \in \mho(\phi^*, r)$.

Finally, we show the uniqueness of the solution. Let ψ^* be another solution. So mathematically, $\Psi(\psi^*) = 0$. For some $\psi^* \in \overline{\mho}(\phi^*, R)$, let $T = \int_0^1 \Psi'(\psi^*+\theta(\phi^*-\psi^*))d\theta$ with $\Psi(\psi^*) = 0$.

$$\begin{aligned}\|(\Psi'(\phi^*))^{-1}\Psi'(\phi^*)-(\Psi'(\phi^*))^{-1}T\| &\leq \int_0^1 \mu_0\|[(\psi^*-\phi^*)+\theta(\phi^*-\psi^*)]\|d\theta \\ &\leq \int_0^1 \mu_0\|(\phi^*-\psi^*)(1-\theta)\|d\theta \\ &< 1.\end{aligned}$$

From this by the Banach lemma, it follows that T is invertible. Then, in view of identity $0 = \Psi(\phi^*)-\Psi(\psi^*) = T(\phi^*-\psi^*)$, we conclude that $\phi^* = \psi^*$. □

3. Basins of attraction

In this section, we discuss the proposed method's basins of attraction based on a visual representation of their basins of attraction when $\Psi(\phi)$ is a given fixed complex polynomial $p(z)$. If ϕ^* is a root of the function $\Psi(\phi)$, then the basins of attraction of ϕ^* are given by the set of all numbers ϕ_0 such that the method starting at ϕ_0 converges to ϕ^*. Mathematically,

$$B(\phi^*) = \{z_0 \in \mathbb{C} : \phi(z) \to \phi^* \text{ as } n \to \infty\}. \tag{3.1}$$

By widening the choice of initial point to the complex plane, we may do further analysis of the suggested method's behavior. Even if the roots of the function are real, we will still find a solution. Drawing the basins of attraction in a figure is the best technique to study the method's behavior in the complex plane. Mathematica software is useful for this purpose. This has been discussed by many researchers; for the details of these concepts see [17–20].

Here again, numerical approaches can help make sense of the complexities of a dynamical system by analyzing the behavior to its foundations and investigating its consequences. Since different approaches produce varying results, it is important to investigate each numerical method separately.

A complex polynomial of order n with different roots divides the complex plane into n basins, although these basins need not be evenly spaced or even connected.

One popular method to visualize these regions is basin coloring. The process just assigns n colors to the n basins runs some numerical method to figure out which initial points within a bounded region or mesh converge to a certain basin, and paints that basin's color to that point. In addition, a range of color intensities can be used to demonstrate the number of iterations required to converge to a root. Points calling for fewer iterations appear with greater intensity. With these methods, meaningful geometric interpretations of nearly all complex polynomials are attainable.

While real and imaginary roots both produce a wide range of basin forms, sizes and complexity, the resulting geometries are strikingly similar, with the only discernible change being a rotation along the appropriate axis. Mixed roots, i.e., those roots containing both real and imaginary components, provide a rich variety of basin shapes, sizes and complexities.

Cayley is generally credited as being the first to think about and explain the existence of a basin of attraction for the complex Newtonian approach. The purpose of this section is to employ this graphical tool in order to illustrate the suggested method's basins. We chose to use the effective computer programming package Mathematica [11.3] to see the basins of attraction for complex functions.

We take a rectangle $\Omega = [-3, 3] \times [-3, 3] \in \mathbb{C}$ of 250×250 points and we apply our iterative methods starting in every zero $z^{(0)}$ in the square. With a maximum of 100 iterations and a tolerance $\left|\phi(z^{(k)})\right| < \times 10^{-4}$ we determine that $z^{(0)}$ is the basin of attraction of this zero if the sequence obtained by the iterative procedures attempts a zero of the polynomial.

Problem 1: Let $P(z) = z^2 + 1$ have the zeros $\{i, -i\}$. From Figure 1, we take into consideration a rectangle $\Omega = [3, 3] \times [-3, 3] \in \mathbb{C}$, and if our iterative technique starting from z_0 does not converge, we mark the point as black; we colorize each point z_0 if it converges. We chose a criterion of less than 10^{-4} as our cutoff for defining when convergence is complete. The Julia set of iteration functions is made up of the common edges of these basins of attraction.

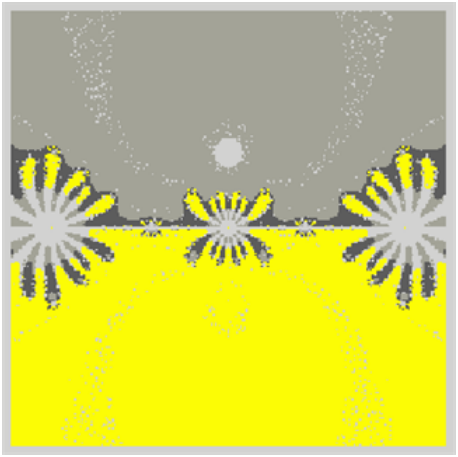

Figure 1. $z^2 + 1$.

Problem 2: Let $P(z) = z^3 + 1$ have the zeros $\{-1, 0.5 - 0.866025i, 0.5 + 0.866025i\}$. In Figure 2, we take into consideration a rectangle $\Omega = [3, 3] \times [-3, 3] \in \mathbb{C}$, and if our iterative technique starting from z_0 does not converge, we mark the point as white; we colorize each point z_0 if it converges. We chose a criterion of less than 10^{-4} as our cutoff for defining when convergence is complete. The Julia set of

iteration functions is made up of the common edges of these basins of attraction.

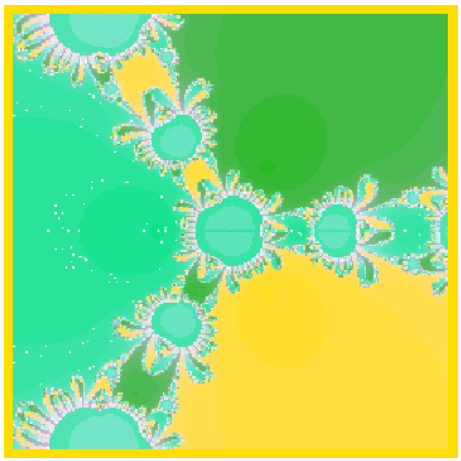

Figure 2. $z^3 + 1$.

Problem 3: Let $P(z) = z^4 + 1$ have the zeros $\{-0.707107 + 0.707107i, -0.707107 - 0.707107i, 0.707107 + 0.707107i, 0.707107 + 0.707107i\}$. In Figure 3, we take into consideration a rectangle $\Omega = [3, 3] \times [-3, 3] \in \mathbb{C}$, and if our iterative technique starting from z_0 does not converge, we mark the point as white; we colorize each point z_0 if it converges. We chose a criterion of less than 10^{-4} as our cutoff for defining when convergence is complete. The Julia set of iteration functions is made up of the common edges of these basins of attraction.

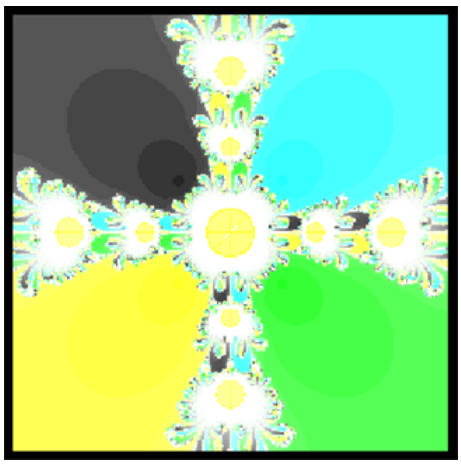

Figure 3. $z^4 + 1$.

Problem 4: Let $P(z) = z^5 + 1$ have the zeros $\{0.809017 + 0.587785i, 0.809017 - 0.587785i, -1, -0.309017+0.951057i, -0.309017-0.951057i\}$. In Figure 4, we take into consideration a rectangle $\Omega = [3, 3] \times [-3, 3] \in \mathbb{C}$, and if our iterative technique starting from z_0 does not converge, we mark the point as light yellow; we colorize each point z_0 if it converges. We chose a criterion of less than 10^{-4} as our cutoff for defining when convergence is complete. The Julia set of iteration functions is made up of the common edges of these basins of attraction.

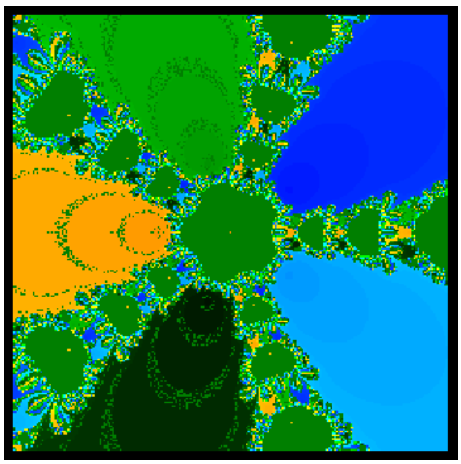

Figure 4. $z^5 + 1$.

Problem 5: Let $P(z) = z^6 + 1$ have the zeros $\{i, -i, -0.866025 + 0.25i, -0.866025 - 0.25i, 0.866025 - 0.25i, 0.866025 - 0.25i\}$. In Figure 5, we take into consideration a rectangle $\Omega = [3, 3]\times[-3, 3] \in \mathbb{C}$, and if our iterative technique starting from z_0 does not converge, we mark the point as black; we colorize each point z_0 if it converges. We chose a criterion of less than 10^{-4} as our cutoff for defining when convergence is complete. The Julia set of iteration functions is made up of the common edges of these basins of attraction.

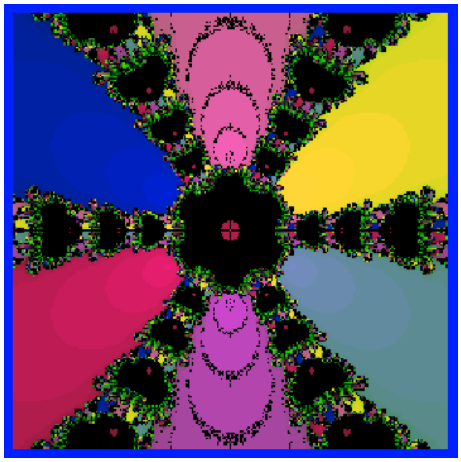

Figure 5. $z^6 + 1$.

Problem 6: Let $P(z) = z^7 + 1$ have the zeros $\{-1, 0.222521 + 0.974928i, 0.222521 + 0.974928i, 0.2349 + 0.781831i, 0.2349 - 0.781831i, 0.900969 + 0.433884i, 0.900969 - 0.433884i\}$. In Figure 6, we consider a rectangle $\Omega = [3, 3] \times [-3, 3] \in \mathbb{C}$, and if our iterative technique starting from z_0 does not converge, we mark the point as light yellow ; we colorize each point z_0 if it converges. We chose a criterion of less than 10^{-4} as our cutoff for defining when convergence is complete. The Julia set of iteration functions is made up of the common edges of these basins of attraction.

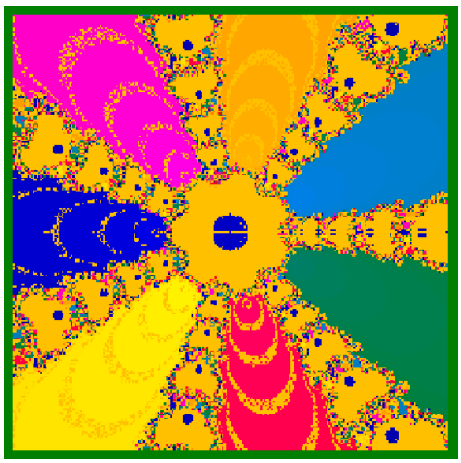

Figure 6. $z^7 + 1$.

Problem 7: Let $P(z) = z^3 - z$ have the zeros $\{-1, 0, 1\}$. In Figure 7, we take into consideration a rectangle $\Omega = [3, 3] \times [-3, 3] \in \mathbb{C}$, and if our iterative technique starting from z_0 does not converge, we mark the point as black; we colorize each point z_0 if it converges. We chose a criterion of less than 10^{-4} as our cutoff for defining when convergence is complete. The Julia set of iteration functions is made up of the common edges of these basins of attraction.

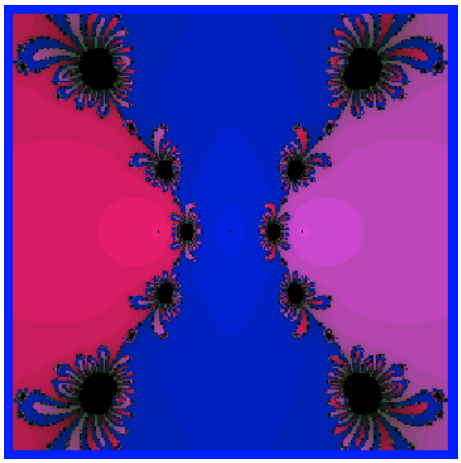

Figure 7. $z^3 - z$.

Problem 8: Let $P(z) = z^4 - 5 * z^2 + 4$ have the zeros $\{-2, -1, 1, 2\}$. In Figure 8, we take into consideration a rectangle $\Omega = [3, 3] \times [-3, 3] \in \mathbb{C}$, and if our iterative technique starting from z_0 does not converge, we mark the point as white; we colorize each point z_0 if it converges. We chose a criterion of less than 10^{-4} as our cutoff for defining when convergence is complete. The Julia set of iteration functions is made up of the common edges of these basins of attraction.

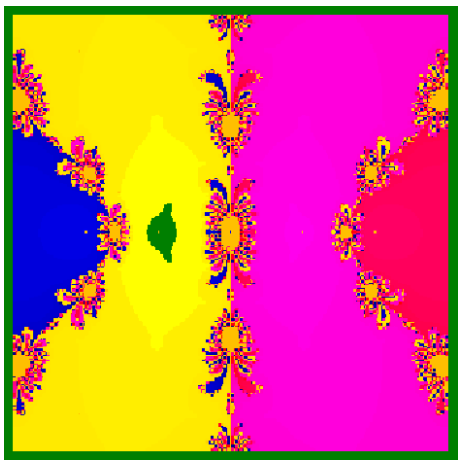

Figure 8. $z^4 - 5 * z^2 + 4$.

Problem 9: Let $P(z) = z^6 + z - 1$ have the zeros $\{-1.13472, -0.451055 + 1.00236i, -0.45105 - +1.00236i, 0.629372 + 0.735756i, 0.629372 - 0.735756i, 0.77809\}$. In Figure 9, we take into consideration a rectangle $\Omega = [3, 3] \times [-3, 3] \in \mathbb{C}$, and if our iterative technique starting from z_0 does not converge, we mark the point as white; we colorize each point z_0 if it converges. We chose a criterion of less than 10^{-4} as our cutoff for defining when convergence is complete. The Julia set of iteration functions is made up of the common edges of these basins of attraction.

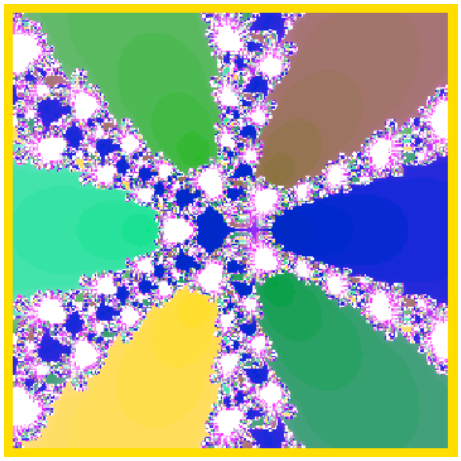

Figure 9. $z^6 + z - 1$.

4. Numerical examples

In this section, some numerical examples are presented to check the efficiency of our method given by Eq (1.5) and denoted by PM; it is also compared with existing sixth order iterative methods [9,21,22], respectively denoted as IS_1, IS_2 and IS_3. We observe that our method gives better results than the existing methods.

Example 4.1. *Take into consideration the Kepler equation, which is defined by* $\Psi : \Omega \subseteq R \to R$

$$\lambda_1 x - \lambda_2 \sin(\phi) - \lambda_3, \tag{4.1}$$

where $\lambda_1 = 1$, $0 \leq \lambda_2 \leq \pi$ and $0 \leq \lambda_3 \leq \pi$. To calculate the radius of the convergence ball, $\mu = \mu_0 = \frac{\lambda_3}{|\lambda_1 - \lambda_2 \cos(\phi^*)|}$ we have used the parameters. By applying Theorem 2.1, in Table 1, we can present different radii of convergence. We compared our proposed method with that in [9].

Table 1. Radius of Convergence results for different values of $\lambda_1, \lambda_2, \lambda_3$.

λ_1	λ_2	λ_3	ϕ^*	r_1	r_2	r_3	$r = \min(r_1, r_2, r_3)(PM)$	r IS$_1$
1	0.4	0.2	0.329386	2.07168	1.25332	0.859141	0.859141	0.139606
1	0.5	0.3	0.569682	1.28569	0.778358	0.533557	0.533557	0.0960825
1	0.6	0.4	0.851271	1.00674	0.609601	0.417876	0.417876	0.0874638
1	0.7	0.5	1.134395	0.938831	0.567974	0.38934	0.38934	0.107392
1	0.8	0.6	1.386444	0.938831	0.567974	0.393213	0.393213	0.140124

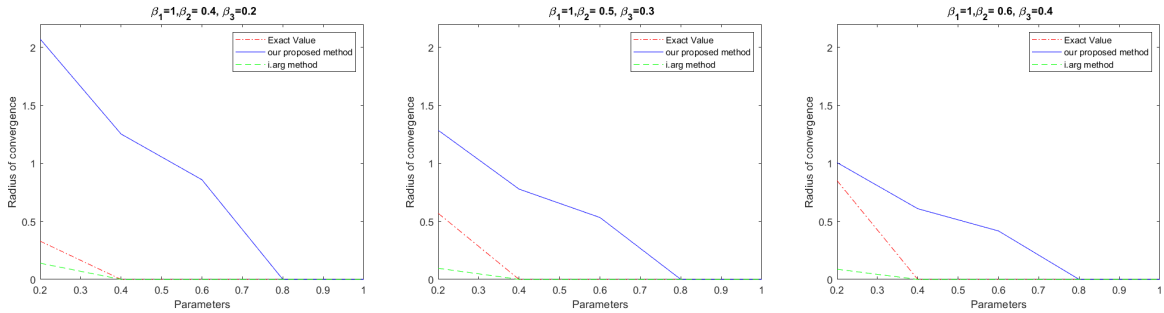

(a) $\lambda_1 = 1, \lambda_2 = 0.4, \lambda_3 = 0.2$ **(b)** $\lambda_1 = 1, \lambda_2 = 0.5, \lambda_3 = 0.3$ **(c)** $\lambda_1 = 1, \lambda_2 = 0.6, \lambda_3 = 0.4$

(d) $\lambda_1 = 1, \lambda_2 = 0.7, \lambda_3 = 0.5$ **(e)** $\lambda_1 = 1, \lambda_2 = 0.8, \lambda_3 = 0.6$

Figure 10. Comparision of radius of convergence for different values of $\lambda_1,\ \lambda_2,\ \lambda_3$.

Example 4.2. *Let the space of continuous functions* $\varphi = \varpi = C[0, 1]$ *have the maximum norm defined on* $[0, 1]$. *Let* $\Omega = \overline{\mho}(0, 1)$ *and on* Ω, *define a function* Ψ *by*

$$\Psi(\phi)(\phi) = \phi(\phi) - 5 \int_0^1 \phi\theta\phi(\theta)^3 d\theta. \tag{4.2}$$

We have that

$$\Psi'(\phi(\epsilon))(\phi) = \epsilon(\phi) - 15 \int_0^1 \phi\theta\phi(\theta)^2 \epsilon(\theta) d\theta,$$

for each $\epsilon \in \Omega$.

Then we get that $\phi^* = 0$, $\mu_0 = 7.5$, $\mu = 15$ and $\kappa = 1 + 7.5t$. We compared our proposed method with [21].

Table 2. Comparison of radius of convergence.

μ_0	μ	κ	r_1	r_2	r_3	r by PM	r IS$_2$
7.5	15	$1 + 7.5t$	0.0666667	0.0600043	0.0305504	0.0305504	0.0065

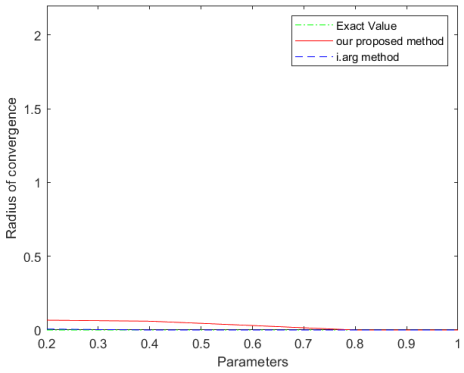

Figure 11. Comparison of radius of convergence.

Example 4.3. *Let* $\Psi : \Omega \subset \mathbb{R} \to \mathbb{R}$ *and consider a nonlinear equation which is defined on* Ψ *by*

$$\Psi(\phi) = \frac{\phi^3}{6} + \frac{\phi^2}{6} - \frac{5\phi}{6} + \frac{1}{3}. \tag{4.3}$$

The approximate root of Eq (4.3) is $\phi^* = 0.46259$ and $\Psi'(\phi^*) = 0.572135$. Then we get $\mu = 0.42385$, $L_0 = 0.45653$. By using the Theorem 2.1, we get the radius of convergence

Table 3. Comparison of radius of convergence.

μ_0	μ	κ	r_1	r_2	r_3	$r = \min(r_1, r_2, r_3)$(PM)	r IS$_2$
0.42385	0.45653	$1 + 0.45653t$	1.53347	0.9880768	0.639473	0.639473	0.367812

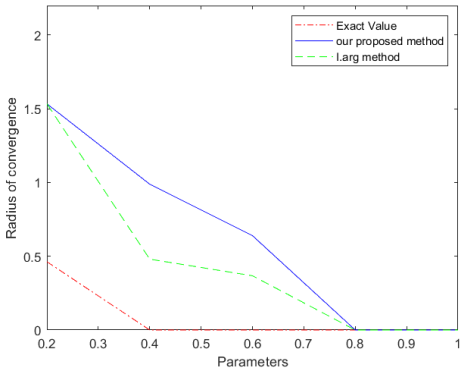

Figure 12. Comparison of radius of convergence.

Example 4.4. *[22] The chemical reactor problem for continuous stirred tank reactors (CSTRs) is analyzed. In order to transmit the reactor's function, Douglas created an easy-to-understand expression:*

$$\rho_c \frac{2.98(\varrho + 2.25)}{(\varrho + 1.45)(\varrho + 2.85)^2(\varrho + 4.35)} = -1, \tag{4.4}$$

where ρ_c is the gain of the proportional controller.

For ρ_c values where the transfer function roots have a negative real portion, the control system is stable. By setting $\rho_c = 0$, we obtain the poles of the open-loop transfer function as the roots of the nonlinear equation.

Here is the nonlinear equation:

$$\varphi(\varrho) = \varrho^4 + 11.50\varrho^3 + 47.49\varrho^2 + 83.06325\varrho + 51.23266875 \tag{4.5}$$

There are four approximate roots of this equation $\varrho^* = -4.35, -2.85, -2.28, -1.45$. We chose out of the four approximate roots -4.35 as the approximate root. We take into consideration $\Omega = [-4.5, -4]$. Then, we obtain that $\mu = \mu_0 = 2.760568793$ *and* $\kappa = 2$.

Table 4. Comparison of radius of convergence.

μ_0	μ	κ	r_1	r_2	r_3	$r = \min(r_1, r_2, r_3)$(PM)	r IS$_3$
2.760568793	2.760568793	2	0.243081	0.123494	0.10068	0.10068	0.0241496

As a result, the Theorem 2.1 allows us to guarantee convergence of the proposed technique.

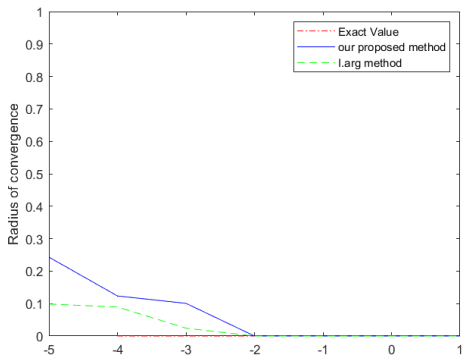

Figure 13. Radius of convergence.

Example 4.5. *[22] An electron's path in the vacuum between two parallel plates is described for the purpose of investigating the multi-factor effect:*

$$\varrho(s) = \varrho_0 + \Big(\lambda_0 + e\frac{E_0}{m\omega}\sin(\omega s_0 + \mu)\Big)(s - s_0) + e\frac{E_0}{m(\omega)^2}\Big(\cos(\omega s + \mu)) + \sin(\omega s_0 + \mu)\Big) \tag{4.6}$$

Where
m = The weight of a stationary electron,

e = The static charge of an electron,
ϱ_0 = Position of the electron at time s_0,
λ_0 = Velocity of the electron at time s_0,
$E_0 \sin(\omega s + \mu)$ = The electric field between the plates as generated by radio waves.

By adjusting some of the parameters in Eq (4.6), we may obtain its simplified form, which is given by

$$\varphi(\varrho) = \varrho - \frac{\cos(\varrho)}{2} + \frac{\pi}{4}; \tag{4.7}$$

$\varrho^* = -0.30909327154179$ is the required root of the function. Then, we have that $\mu_0 = 1.523542095$, $\mu = 1.523542095$ and $\kappa = 1.523542095$. Then by using the g functions, we get

Table 5. Comparison of radius of convergence.

μ_0	μ	κ	r_1	r_2	r_3	$r = \min(r_1, r_2, r_3)$(PM)	r IS$_3$
1.523542095	1.523542095	1.523542095	0.437577	0.218788	0.181466	0.181466	0.170313

As a result, Theorem 2.1 allows us to guarantee convergence of the proposed technique.

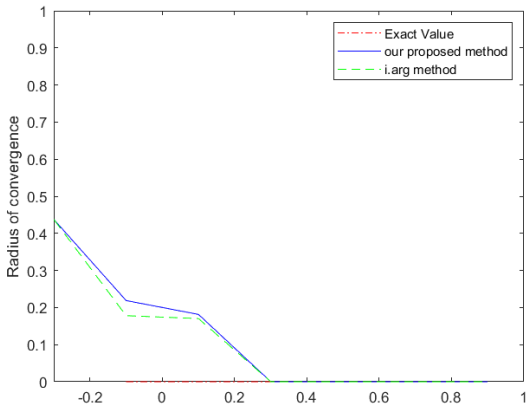

Figure 14. Comparison of radius of convergence.

5. Conclusions

In this paper, we looked at the research into the local convergence of the sixth-order iterative approach with parameters. In this study, we use the assumption that the first-order Fréchet derivative fulfills the Lipschitz continuity requirement. As a result of this work, we also provided the theoretical radius of convergence. Finally, some numerical examples are given to illustrate how the results of our research can be utilized to compute the radius of the convergence ball to solve nonlinear equations. Also, we noticed that our radius of the convergence ball is larger than the one that was already there. This method's behavior reveals a less chaotic, more attractive basin of attraction.

Use of AI tools declaration

The authors declare they have not used Artificial Intelligence (AI) tools in the creation of this article.

Conflict of interest

The authors declare that they have no competing interests.

References

1. C. Chun, B. Neta, Developing high order methods for the solution of systems of nonlinear equations, *Appl. Math. Comput.*, **342** (2019), 178–190. https://doi.org/10.1016/j.amc.2018.09.032
2. H. Montazeri, F. Soleymani, S. Shateyi, S. S. Motsa, On a new method for computing the numerical solution of systems of nonlinear equations, *J. Appl. Math.*, **2012** (2012), 751975. https://doi.org/10.1155/2012/751975
3. S. Abbasbandy, P. Bakhtiari, A. Cordero, J. R. Torregrosa, T. Lotfi, New efficient methods for solving nonlinear systems of equations with arbitrary even order, *Appl. Math. Comput.*, **287–288** (2016), 94–103. https://doi.org/10.1016/j.amc.2016.04.038
4. I. K. Argyros, Á. A. Magreñán, A study on the local convergence and the dynamics of Chebyshev-Halley-Type methods free from second derivative, *Numer. Algor.*, **71** (2016), 1–23. http://doi.org/10.1007/s11075-015-9981-x
5. L. V. Kantorovich, G. P. Akilov, *Functional analysis*, Oxford: Pergamon Press, 1982. https://doi.org/10.1016/C2013-0-03044-7
6. L. B. Rall, *Computational solution of nonlinear operator equations*, New York: Robert E. Krieger, 1979.
7. A. S. Alshomrani, R. Behl, P. Maroju, Local convergence of parameter based method with six and eighth order of convergence, *J. Math. Chem.*, **58** (2020), 841–853. https://doi.org/10.1007/s10910-020-01113-6
8. I. K. Argyros, S. George, Local convergence for an almost sixth order method for solving equations under weak conditions, *SeMA*, **75** (2018), 163–171. https://doi.org/10.1007/s40324-017-0127-z
9. I. K. Argyros, S. K. Khattri, S. George, Local convergence of an at least sixth-order method in Banach spaces, *J. Fixed Point Theory Appl.*, **21** (2019), 23. https://doi.org/10.1007/s11784-019-0662-6
10. P. Maroju, Á. A. Magreñán, Í. Sarría, A. Kumar, Local convergence of fourth and fifth order parametric family of iterative methods in Banach spaces, *J. Math. Chem.*, **58** (2020), 686–705. https://doi.org/10.1007/s10910-019-01097-y
11. S. Singh, E. Martínez, P. Maroju, R. Behl, A study of the local convergence of a fifth order iterative method, *Indian J. Pure Appl. Math.*, **51** (2020), 439–455. https://doi.org/10.1007/s13226-020-0409-5
12. I. K. Argyros, S. George, Local convergence of deformed Halley method in Banach space under Holder continuity conditions, *J. Nonlinear Sci. Appl.*, **8** (2015), 246–254. http://doi.org/10.22436/jnsa.008.03.09
13. A. A. Magrenãn, I. K. Argyros, On the local convergence and the dynamics of Chebyshev-Halley methods with six and eight order of convergence, *J. Comput. Appl. Math.*, **298** (2016), 236–251. https://doi.org/10.1016/j.cam.2015.11.036

14. A. S. Alshomrani, R. Behl, P. Maroju, Local convergence of parameter based method with six and eighth order of convergence, *J. Math. Chem.*, **58** (2020), 841–853. https://doi.org/10.1007/s10910-020-01113-6

15. J. R. Sharma, R. K. Guha, R. Sharma, An efficient fourth order weighted-Newton method for systems of nonlinear equations, *Numer. Algor.*, **62** (2013), 307–323. https://doi.org/10.1007/s11075-012-9585-7

16. F. Soleymani, Regarding the accuracy of optimal eighth-order methods, *Math. Comput. Model.*, **53** (2011), 1351–1357. https://doi.org/10.1016/j.mcm.2010.12.032

17. M. Scott, B. Neta, C. Chun, Basins attractors for various methods, *Appl. Math. Comput.*, **218** (2011), 2584–2599. https://doi.org/10.1016/j.amc.2011.07.076

18. R. Behl, P. Maroju, S. S. Motsa, A family of second derivative free fourth order continuation method for solving nonlinear equations, *J. Comput. Appl. Math.*, **318** (2017), 38–46. https://doi.org/10.1016/j.cam.2016.12.008

19. R. Behl, S. S. Motsa, Geometric construction of eighth-order optimal families of Ostrowski's method, *Sci. World J.*, **2015** (2015), 614612. https://doi.org/10.1155/2015/614612

20. S. M. Kang, S. M. Ramay, M. Tanveer, W. Nazeer, Polynomiography via an iterative method corresponding to Simpsons 1/3 rule, *J. Nonlinear Sci. Appl.*, **9** (2016), 967–976. http://doi.org/10.22436/jnsa.009.03.25

21. I. K. Argyros, S. George, Local convergence of deformed Halley method in Banach space under Holder continuity conditions, *J. Nonlinear Sci. Appl.*, **8** (2015), 246–254. http://doi.org/10.22436/jnsa.008.03.09

22. A. S. Alshomrani, I. K. Argyros, R. Behl, An optimal reconstruction of Chebyshev-Halley-Type methods with local convergence analysis, *Int. J. Comp. Meth.*, **17** (2020), 1940017. https://doi.org/10.1142/S0219876219400176

AIMS Press